



Contents lists available at ScienceDirect

Ceramics International

journal homepage: www.elsevier.com/locate/ceramint

Study on the Five dynasty sky-green glaze from Yaozhou kiln and its coloring mechanism

Pei Shi, Fen Wang*, Jianfeng Zhu, Biao Zhang, Ting Zhao, Yi Wang, Yi Qin

School of Materials Science and Engineering, Shaanxi University of Science & Technology, Xi'an 710021, PR China

ARTICLE INFO

Keywords:

Yaozhou kiln
Five dynasty
Sky-green glaze
Celadon
Tongchuan
Shannxi province

ABSTRACT

This work takes the Five dynasty sky-green glaze of Yaozhou kiln as the major study object. Based on the analysis of XRF, XRD, XPS and SEM/EDS, the chemical compositions, firing technique and microstructure of the sky-green glaze were investigated. A possible coloring mechanism was proposed to explain the variation of glaze appearance. The results indicated that the Five dynasty sky-green glaze had relatively high contents of CaO and K₂O, which led to the better gloss and transparency than others. Besides that, the chemical coloring of Fe₂O₃ and the scattering of physical structures also affected the color saturation and opacity of glaze surface. The high Fe²⁺/Fe³⁺ ratio and phase separation droplets of forming structural color by the amorphous photons and Rayleigh scattering contributed to increasing the blue tone of sky-green glaze. In addition, the residual crystals decreased the transparency of glaze surfaces.

1. Introduction

The Yaozhou kiln in the Huangpu town of the Shaanxi province of China had a long history of producing celadon wares. The Yaozhou celadon started from the Tang dynasty (618 AD–917 AD), passed through the Five dynasty (907 AD–960 AD), matured in the Song

dynasty (960 AD–1279 AD) and stopped development in the Yuan dynasty (1279 AD–1368). The history of its continuous production had persisted for nearly 800 years [1,2].

At first, the Yaozhou celadon was appreciated for the Song dynasty celadon with carved decoration (Fig. 1(a)). Nevertheless, the awareness about the Five dynasty celadon had been going on for quite a long time.

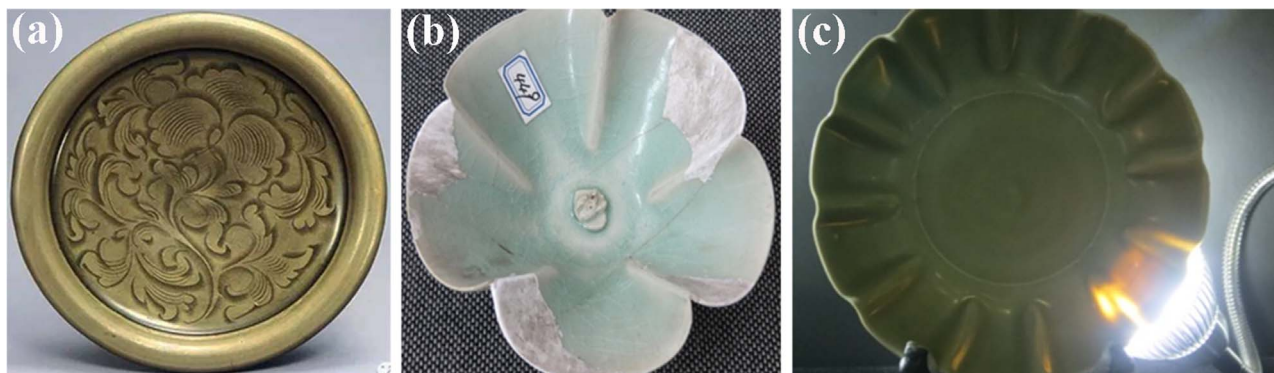


Fig. 1. (a) Song dynasty celadon with carved decoration; (b) and (c) Five dynasty sky-green ware.

* Corresponding author.

E-mail address: wangf@sust.edu.cn (F. Wang).

<http://dx.doi.org/10.1016/j.ceramint.2016.11.019>

Received 28 October 2016; Received in revised form 3 November 2016; Accepted 4 November 2016

Available online xxx

0272-8842/ © 2016 Elsevier Ltd and Techna Group S.r.l. All rights reserved.

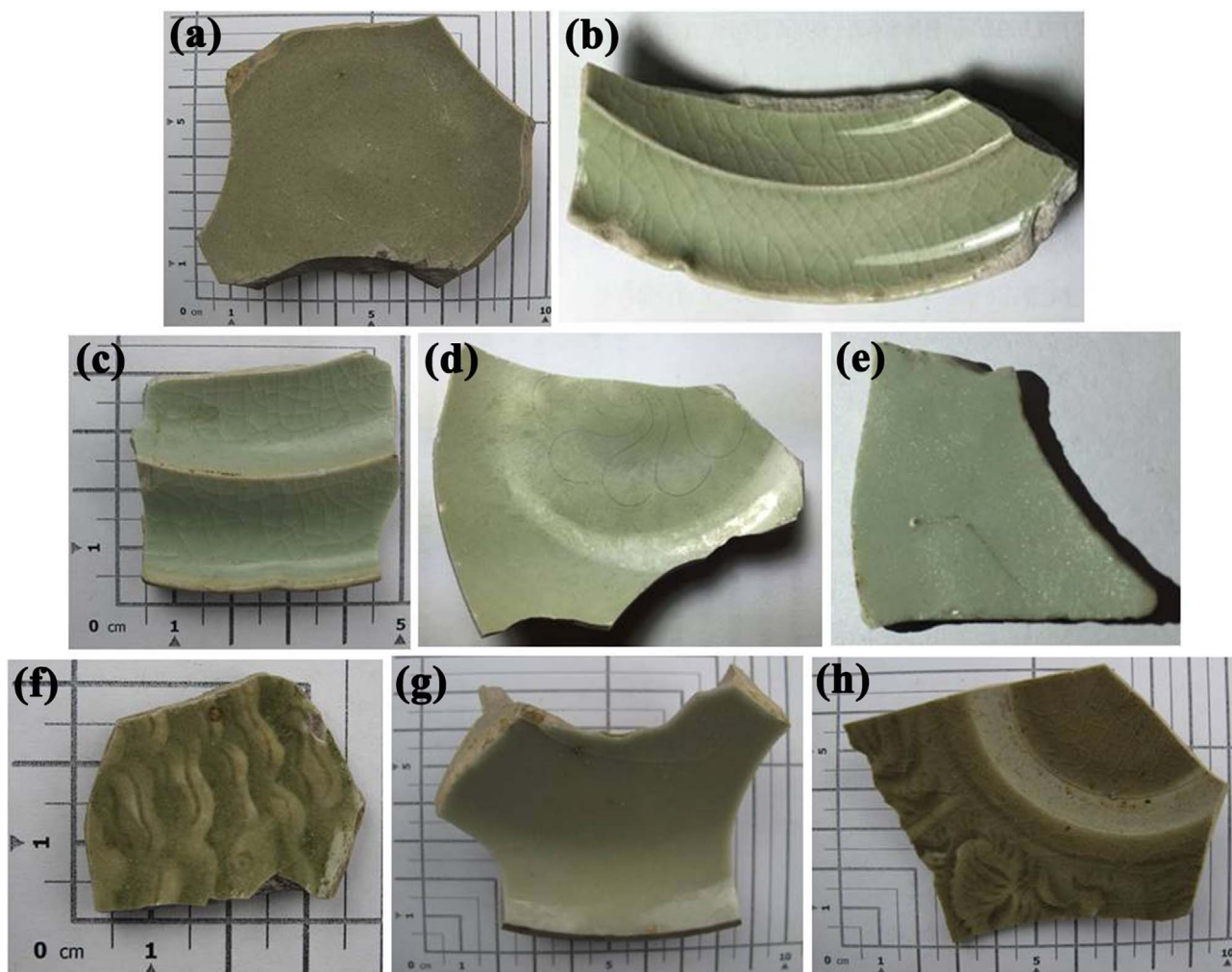


Fig. 2. Appearance of celadon shards of different dynasties, (a) T1; (b)–(e) W1–W4; (f) S1; (g) J1; (h) Y1.

Table 1

Chemical compositions of the shards from different dynasties (wt%).

| Number | Dynasty | Na ₂ O | MgO | Al ₂ O ₃ | SiO ₂ | K ₂ O | CaO | TiO ₂ | Fe ₂ O ₃ |
|--------|--------------|-------------------|------|--------------------------------|------------------|------------------|-------|------------------|--------------------------------|
| T1 | Tang | 0.44 | 2.48 | 12.63 | 67.34 | 2.25 | 12.30 | 0.12 | 1.45 |
| T2 | | 0.24 | 2.32 | 13.24 | 61.55 | 2.42 | 16.92 | 0.23 | 2.09 |
| T3 | | 0.37 | 1.68 | 13.18 | 65.71 | 2.19 | 13.99 | 0.08 | 1.80 |
| W1 | Five dynasty | 0.29 | 1.49 | 12.08 | 70.41 | 3.50 | 9.34 | 0.11 | 1.78 |
| W2 | | 0.34 | 1.26 | 11.58 | 66.83 | 3.66 | 13.27 | 0.09 | 1.98 |
| W3 | | 0.24 | 1.32 | 13.96 | 68.82 | 5.88 | 6.62 | 0.13 | 2.03 |
| W4 | | 0.07 | 1.58 | 12.39 | 69.39 | 3.59 | 10.07 | 0.09 | 1.83 |
| S1 | Song | 0.51 | 1.79 | 12.90 | 69.56 | 2.75 | 9.48 | 0.11 | 1.92 |
| S2 | | 0.40 | 1.52 | 13.48 | 69.79 | 3.20 | 8.43 | 0.18 | 2.00 |
| S3 | | 0.56 | 1.51 | 13.02 | 72.56 | 3.13 | 6.03 | 0.12 | 2.06 |
| J1 | Jin | 0.24 | 2.09 | 13.31 | 71.44 | 2.66 | 7.33 | 0.12 | 1.81 |
| J2 | | 0.18 | 1.74 | 13.49 | 72.90 | 2.86 | 5.73 | 0.11 | 1.99 |
| J3 | | 0.27 | 1.23 | 14.61 | 73.42 | 3.21 | 4.18 | 0.14 | 1.94 |
| Y1 | Yuan | 0.43 | 0.95 | 15.39 | 73.03 | 2.98 | 4.84 | 0.13 | 1.26 |
| Y2 | | 0.46 | 1.22 | 16.14 | 72.44 | 2.91 | 4.04 | 0.13 | 1.66 |
| Y3 | | 0.56 | 1.62 | 15.70 | 73.22 | 3.72 | 1.64 | 0.13 | 2.42 |

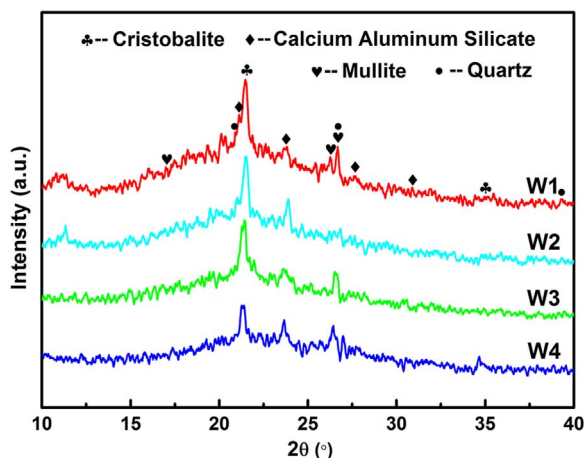


Fig. 3. XRD patterns of sky-green glazes.

At the beginning of this century, a lot of Five dynasty celadon shards of Yaozhou kiln were unearthed in renovation of the Xi Dajie of Xi'an, accompanying with unearthed findings of the Huangpu town and some tombs (Lv's tomb and Liaoning's tomb, etc). Before that, no one had appreciated the Five dynasty celadon although it was so beautiful and high-quality. Especially, the sky-green ware was mirror-like bright, paper-like thin and chime-like sound (Fig. 1(b)–(c)) [1]. In recent years, some researchers [3] claimed that the Five dynasty Yaozhou celadon belonged to the Chai ware, whereas the kiln site had not yet been found. Hence, this view still needed to be demonstrated with convincing archaeological data. Nevertheless, it was now known that the sky-green ware was fired for the first time in the Yaozhou kiln from Five dynasty, while it was also the best Chinese celadon ever found before the Five dynasty.

Previous studies about other dynasties Yaozhou celadon have had endless stream of research results. Chen et al. [4] investigated that the glaze layer of Tang dynasty celadon having a relatively high content of CaO showed high transparency, and the glaze color was mainly gray-green. Li et al. [5] found that in the Northern Song celadon glaze, the

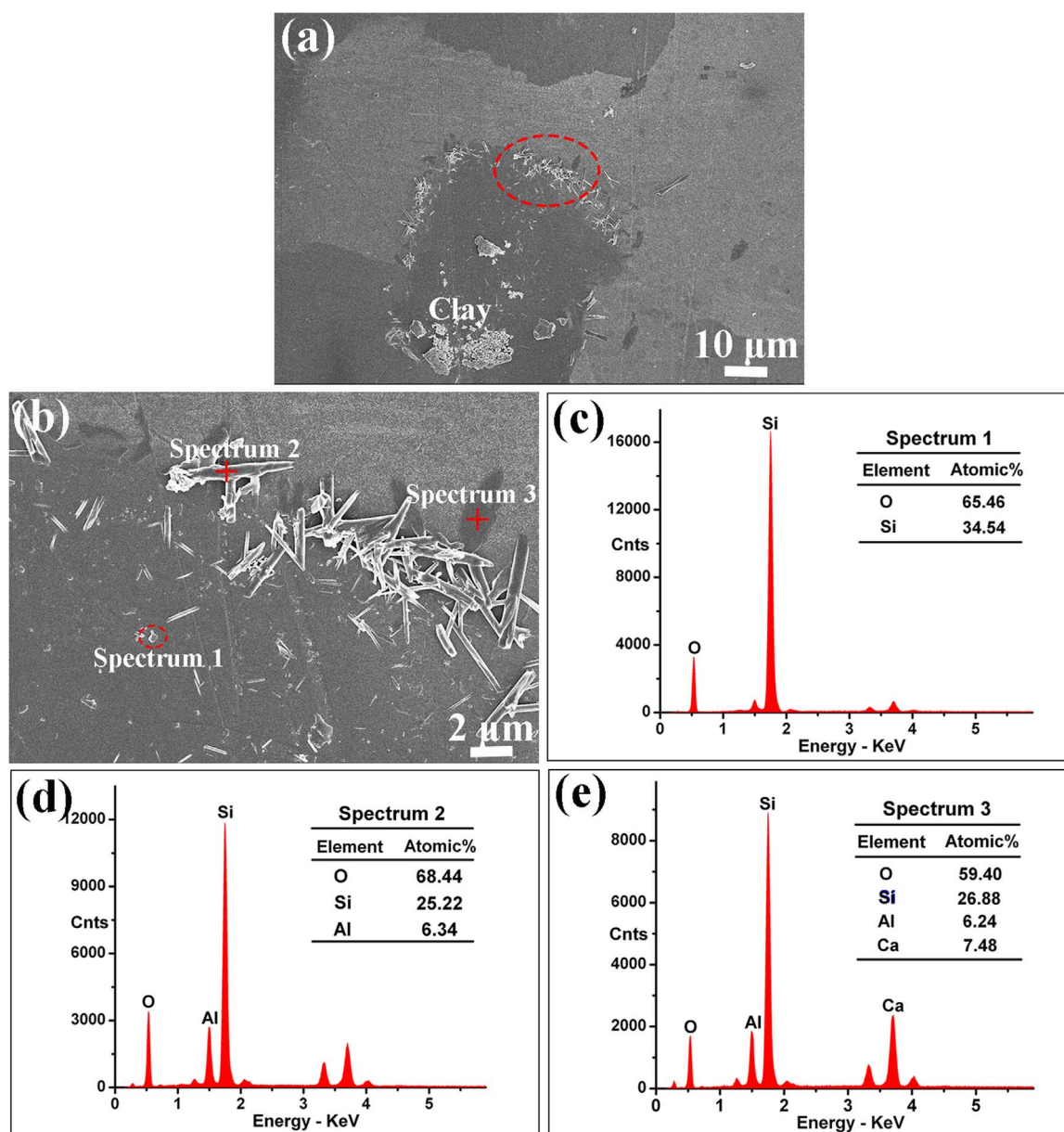


Fig. 4. (a) SEM images of crystals on the W3 glaze surface; (b) enlarged image of (a); (c)–(e) EDS spectra.

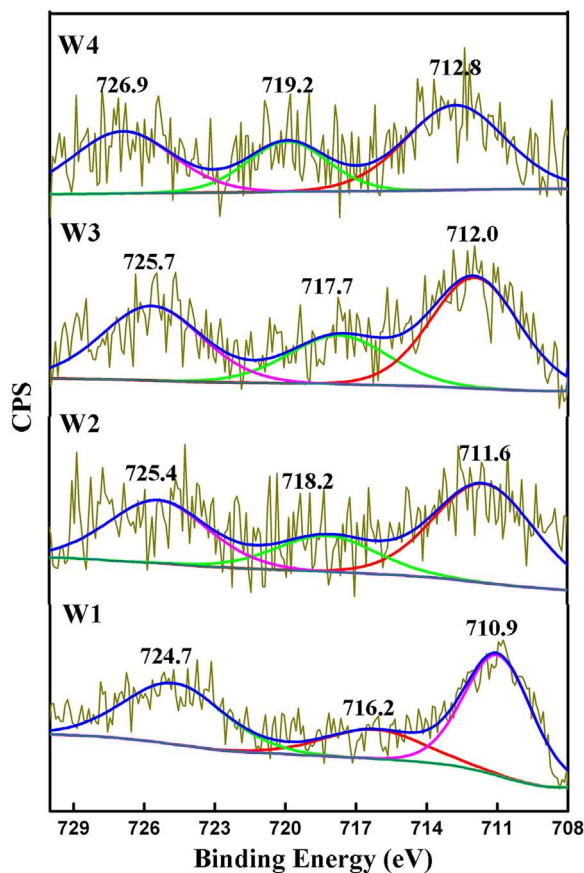


Fig. 5. Fitting XPS spectra of the Fe2p with different samples.

molar ratio of SiO_2 to Al_2O_3 was 8.0–9.0, and it had a lower K_2O but higher TiO_2 content than Longquan kiln. As a result, the Yaozhou celadon glaze in Northern Song mostly appeared olive-green, and the glaze color of Longquan celadon was emerald. Besides, Zhu et al. [6] investigated that the glaze layer of Northern Song celadon was usually thicker (0.25–0.30 mm) than the Xicun kiln. And due to many different sizes of bubbles (0.15–0.2 mm) in the glaze, the opacity of glaze layer was low. In Wang et al.'s study, the Jin dynasty moon-white glaze had relatively high SiO_2 and Al_2O_3 contents but low CaO content [2] and presented a lot of bubbles and residual crystals, causing the highest opacity of glaze surface than that of other dynasties. However, in addition to some archaeological reports, there is no special scientific research report about the Five dynasty sky-green ware with white body (suspected the Chai ware).

In this paper, the chemical compositions, firing conditions and microstructures of the Five dynasty sky-green glaze were studied, aiming at investigating the correlation between them and the glaze appearance. Based on that, the scientific rules behind the aesthetically pleasing appearance of the Yaozhou sky-green glaze of Five dynasty was proposed. This work will throw some light on the better understanding of the coloring mechanism about the Five dynasty sky-green glaze.

2. Experimental procedure

All of the celadon shards excavated from the Yaozhou kiln site of Tongchuan were provided by the Yaozhou kiln museum of Shanxi province. The chemical compositions of shards were determined by X-ray fluorescence (XRF, AXIOS, Netherlands). The phase compositions of the test pieces were identified by X-ray diffraction (XRD, D/max 2200PC, Japan) with $\text{Cu K}\alpha$ radiation ($\lambda=1.5406 \text{ \AA}$) and scanning from

10° to 40° under 40 kV and 100 mA. The scanning rate was $8^\circ/\text{min}$ for 2θ . The chemical analysis was performed on an ESCALAB MKII X-ray photoelectron spectrometer (XPS, VG Scientific, UK) using $\text{Al K}\alpha$ radiation. Microstructure and phase composition were studied by using scanning electron microscopy (SEM, S4800, Japan) equipped with an energy dispersive spectrometry (EDS). Before the testing, the surfaces of the samples were etched in 1 vol% HF for 20 s to expose the crystals and phase separation structures.

3. Results and discussion

Fig. 2 shows the appearance of celadon shards of Tang, Five dynasty, Song, Jin and Yuan dynasty. As being observed, the glossiness and transparency of the Five dynasty sky-green glaze layers were higher than that of other dynasties, and the glaze surfaces presented darker blue tone. The chemical compositions of these celadon glazes from different dynasties are listed in Table 1. For comparison, the Five dynasty sky-green glaze should be classed as high temperature SiO_2 -CaO- K_2O glazes containing high contents of CaO and K_2O ($0.76 < \text{RO}/(\text{RO}+\text{R}_2\text{O}) \leq 0.50$), which led to better glossiness and transparency than others [7]. Furthermore, the relatively higher content of K_2O helped to make the glaze color get bluer. For these reasons, the Five dynasty sky-green glaze had the color of the sky after rain, which pioneered the production of high K_2O glaze. In addition to the chemical compositions, the glaze color variations also came from the fluctuation of firing conditions such as firing temperature and atmosphere. The sky-green glaze of Five Dynasty was fired under high firing temperature (1280–1310 $^\circ\text{C}$) and strong reducing atmosphere in the horse-shoe kiln with wood as fuel [5].

Since the physical appearance were greatly influenced by the crystallization behavior of glazes, it was necessary to clarify the formation of various crystalline phases created in the ancient sky-green glazes. Fig. 3 shows the XRD patterns of the W1–W4 glazes. The characteristic amorphous hump could be seen within the $2\theta=15\text{--}35^\circ$ range in all samples, which were associated to a large amount of aluminosilicate glass [8]. Some crystallization peaks, corresponding to high-cristobalite (SiO_2 , PDF#76-0932), calcium aluminum silicate ($\text{CaAl}_2\text{Si}_2\text{O}_8$, PDF#05-0528), mullite ($3\text{Al}_2\text{O}_3 \cdot 2\text{SiO}_2$, PDF#79-1275) and quartz (SiO_2 , PDF#86-2237) crystallization, were also detected in every sample. Among them, the high-cristobalite and mullite were probably from the decomposition of clay (raw material for the glaze preparation), while the quartz was probably from the starting composition. Besides, the calcium aluminum silicate was probably crystallized from the reaction of CaO, Al_2O_3 and SiO_2 . One can notice that the intensity of the crystallization peaks increased from W1 to W4 glazes. The higher the crystalline content, the lower the transparency. Consequently, the transparency of glaze surfaces gradually decreased.

Fig. 4 displays the SEM images and EDS analyses of the etched W3 glaze surface. It could be clearly seen that a large number of bulk, needle-shaped and lamellar crystals disorderly distributed around the residual crystals (Fig. 4(a)). The chemical composition of crystals was analyzed by EDS in Fig. 4(c), (d) and (e), measured on the microspots denoted by the position 1, 2 and 3 in the SEM image (Fig. 4(b)). It showed that the crystal in position 1 was rich in O and Si, whereas the crystals in position 2 and 3 were rich in O, Si and Al. Furthermore, the atomic ration of Ca was also relatively high in position 3. Combining with the XRD analysis in Fig. 3, position 1 and 2 were high-cristobalite and mullite, which were from the decomposition of clay, while position 3 was nearly calcium aluminum silicate.

The XPS technique is especially powerful for elemental analysis, as the binding energy values of core levels are, to a certain extent dependent on the molecular environment [9]. Hence, XPS was carried out to analyze the stoichiometry and bonding states of the Five dynasty sky-green glazes. Typical broad-scan XPS spectra of the W1–W4 within the binding energy range of 730–708 eV are illustrated in Fig. 5. In the fitting curve, the Fe 2p spectra contained two peaks of Fe 2p_{1/2} and Fe

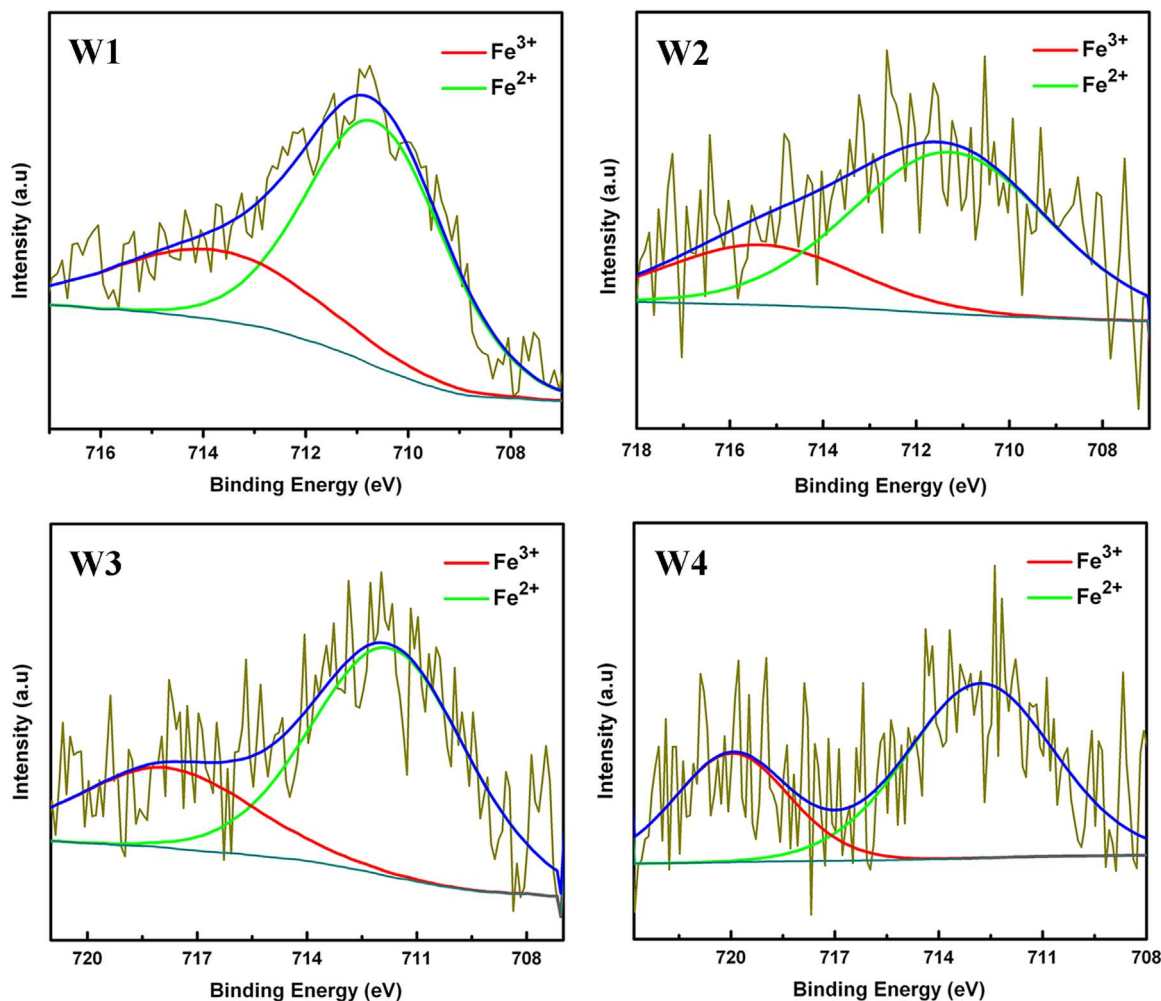


Fig. 6. Fitting XPS spectra of the Fe 2p_{3/2} with different samples.

2p_{3/2} located at the binding energy positions of 710.9–712.8 eV and 724.7–726.9 eV, respectively. In addition, the Fe 2p_{3/2} peak at 716.2–719.2 eV was associated with satellite peaks. For comparison, the binding energy difference between Fe 2p_{1/2} and Fe 2p_{3/2} peaks in every sample around 14 eV indicated the presence of a low oxidation state of iron, while the satellite peak between Fe 2p_{1/2} and Fe 2p_{3/2} confirmed the presence of Fe²⁺ ions [10,11]. It could also be seen from the spectra that the binding energy positions of Fe 2p_{1/2} and Fe 2p_{3/2} gradually shifted to higher binding energy side from W1 to W4. This means that the oxidation state of iron oxide has been changed [11].

Fig. 6 shows the fitted Fe 2p_{3/2} spectra of W1–W4. For every sample, the 2p_{3/2} envelopes were fitted well with the Gaussian multiplets, as well as the multiplets and surface peaks used to fit the Fe³⁺ and Fe²⁺ were labeled on the spectrum. Moreover, the mean relative areas of each constituent peak assigned to Fe²⁺ and Fe³⁺ were calculated. Based on the ratio of relative peak areas, the Fe²⁺ to Fe³⁺ atomic ratios of W1–W4 were 85.00/15.00, 73.99/26.01, 71.73/28.27 and 70.37/29.63 respectively. Therefore, the Fe²⁺ content continuously decreased in W1–W4. Combining with the appearance of samples in Fig. 2(b)–(e), the XPS results confirmed that the Fe²⁺ was helpful to increase the blue tone of sky-blue glaze [12]. Moreover, the sky-green glaze of Five dynasty Yaozhou kiln was fired under strong reducing atmosphere. In order to research the influence of liquid-liquid phase separation on the glaze colors, the W2 and W3 glaze need to be further analyzed.

Fig. 7 presents the SEM micrographs of W2 and W3 glaze surfaces. It could be seen that the discrete droplet phase separation structures

were formed in every sample. Specifically in Fig. 7(a) and (b), the nano-sized phase separation droplets were closely arranged in the W2 glaze surface. While as depicted in Fig. 7(c) and (d), calcium aluminum silicate columns crystals sparsely dispersed without border on each other, and the empty space between these crystals was filled with phase separation droplets.

The formation process of liquid-liquid phase separation was complicated, influenced by the variations in chemical composition, viscosity of the melt, and firing temperature. Whatever small discrete droplet phase separation structures or interconnected phase separation structures were formed in the system of little-viscosity, they would shrink firstly and then grow into large phase separation droplets [13]. Due to the higher CaO content (13.27 wt%) in W2 than in W3, the resulted lower viscosity facilitated the formation and growth of phase separation droplets. However, with further growth of calcium aluminum silicate (Fig. 7(c) and (d)), Al₂O₃ in the circumjacent glass should be consumed greatly followed by a rapid compositional shift into the metastable liquid-liquid immiscibility region above 950 °C with a dramatic rising of the SiO₂/Al₂O₃ ratio. In the local region of low Al₂O₃ concentration, the tendency towards liquid-liquid immiscibility increased with increasing the SiO₂/Al₂O₃ ratio [14]. Additionally, the discrete droplet phase separation structures filled the empty space between the crystals in the W3 surface.

The glaze colors of the Five dynasty Yaozhou celadon is famous primarily for the subtle beauty of its neat and simple glaze, presenting the soft and aesthetically pleasing colors described as sky-green, pink-green, light blueish and light green etc. [15]. Generally, under a certain

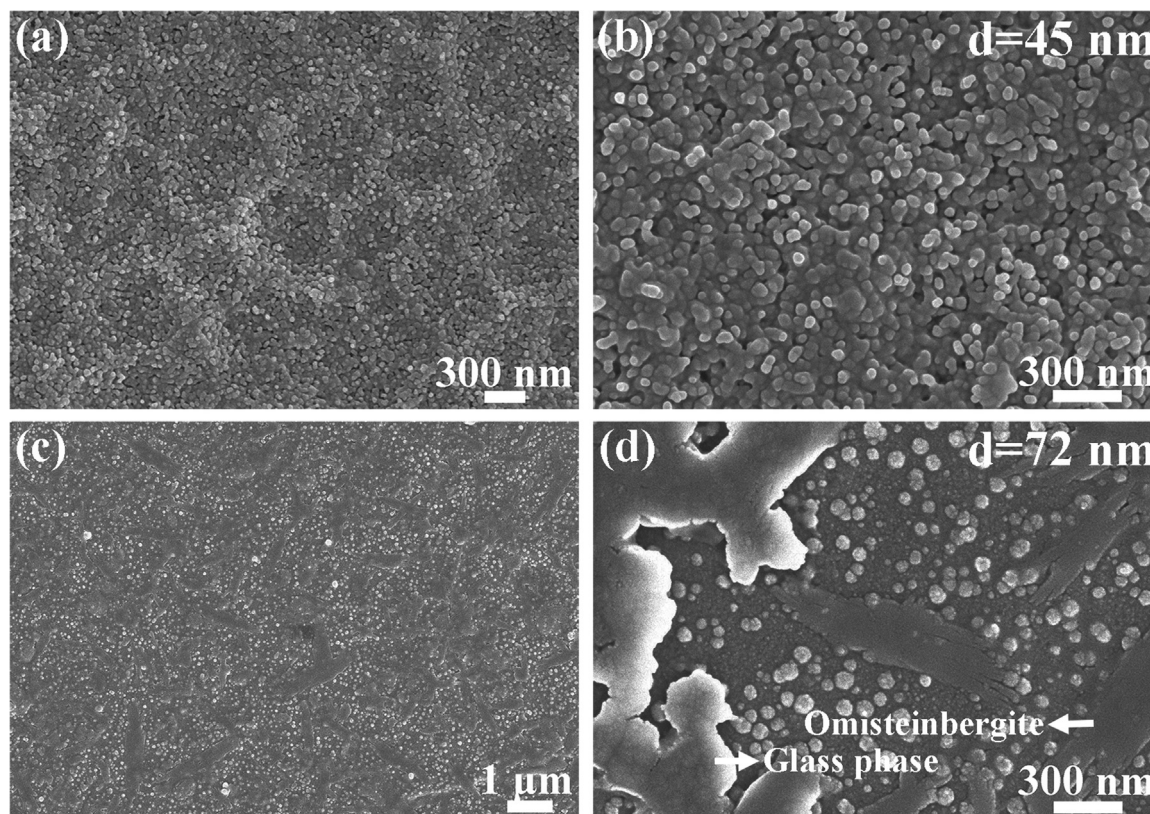


Fig. 7. Typical SEM microstructures of separation structures in the sample surfaces, (a) and (b) W2; (c) and (d) W3.

firing temperature and atmosphere, the variations in hue, saturation of color and opacity are based on the iron as the primary coloring constituent, and also depended on the diffuse reflection and refraction caused by optical inhomogeneities within glaze layers [14].

Structural colors of objects are caused by optical effects such as interference, diffraction, and reflection when the size range of the objects is comparable to the optical wavelength range [16]. According to the coherence between light and object structures, the generating mechanism of structural colors is classified as coherent scattering and incoherent scattering. Based on the translational symmetry of the structure, the coherent light scattering could also be classified as the coherent light of ordered structure (photonic crystal) and the coherent light of disordered structure (amorphous photons). When the coherent incident light moves through the medium, and the coherence of light has mostly or almost lost, this process is known as incoherent scattering (Rayleigh scattering and Mie scattering) [17]. Because blue light is at the short wavelength end of the visible spectrum, it is scattered in the atmosphere much more than the longer-wavelength red light [18,19]. As a result, the structural color developed by the amorphous photons and Rayleigh scattering showed blue and the glaze colors became bluer. Classification and comparison of structural color

Table 2
Classification and comparison of structural color.

| Scattering | Coherent scattering | | Incoherent scattering | |
|----------------|---------------------|----------------------|-----------------------|-------------------|
| Classification | Photonic crystal | Amorphous photons | Rayleigh scattering | Mie scattering |
| Character | Complete order | Short-range order | Complete disorder | Complete disorder |
| Condition | Dense structure | Dense structure | $d < 100$ nm | $d > 100$ nm |
| Effect | Rainbow effect | Bright and mild blue | Blue opalescence | Milk white |

are given in Table 2.

The two-dimensional Fourier transform (2D FT) technique enables a quantitative interpretation of the arrangement of the liquid-liquid phase separation structures [20]. Fig. 8 shows the 2D FT of the SEM images in Fig. 7(b) and (d). From Fig. 8(a), the ring-shaped 2D FT image clearly indicated that the phase separation droplets of W2 substantially nanostructured with respect to visible wavelengths at intermediate spatial frequencies rather than randomly distributed (fully disordered). This short-range ordered structure enabled to form the coherent scattering of visible light. As shown in Fig. 8(b), there was not a circular ring around the origin, which indicated that the phase separation droplets of W3 were completely disordered. The disordered structure enabled to form the incoherent scattering of visible light [19–21]. Based on the above analysis, the structural color of the W2 glaze surface developed by the amorphous photons showed bright and mild blue, whereas the structural color of the W3 glaze surface developed by the Rayleigh scattering showed weak blue opalescence.

4. Conclusion

The Five dynasty sky-green ware shards of Yaozhou kiln excavated from the Yaozhou kiln site of Tongchuan were adopted as test samples. According to the XRF results, the Five dynasty sky-green glaze pioneered the production of high K_2O glaze. Meanwhile, high contents of CaO and K_2O increased the gloss and transparency of glaze surfaces. The color variability was related to the Fe^{2+}/Fe^{3+} ratio of glass and the relative amounts of the structural inhomogeneities resulting from the differences in firing temperature and atmosphere at the different positions of the chamber kiln. The sky-green glaze was fired under strong reducing atmosphere, causing a high ratio of Fe^{2+} and Fe^{3+} (85.00/15.00–70.37/29.63) and the bluer chemical color. Furthermore, there were the phase separation droplets of short-range order and complete disorder in the sky-green glaze, while they formed blue structural color by the amorphous photons and Rayleigh scatter-

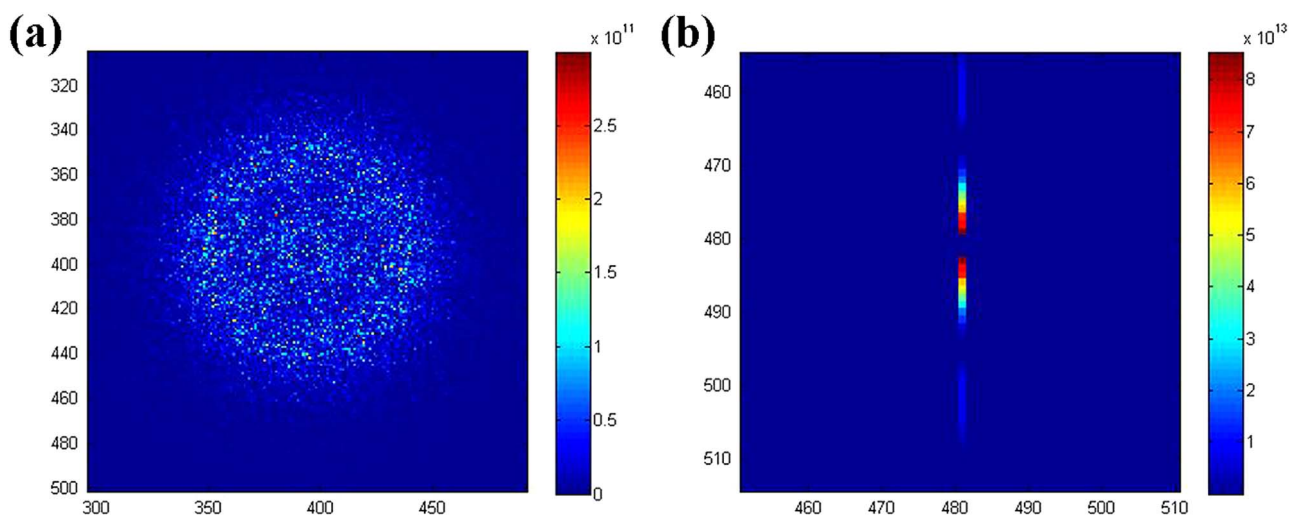


Fig. 8. 2D FT of the SEM images, (a) W2; (b) W3.

ing. The iron content and its reducing/oxidizing state were the main coloring factor, and the structural color formed by phase separation droplets acted as the auxiliary coloring in the glaze.

Acknowledgements

This work was supported by the National Foundation of Natural Science, China (51472153 and 51502165), the Key Project of State Administration of Culture Heritage, China (20120218) and the Graduate Innovation Fund of Shaanxi University of Science and Technology.

References

- [1] J.Z. Li, History of Ancient Science and Technology (Ceramics Part), Science Press, Beijing, 1998.
- [2] F. Wang, Pottery and Porcelain of Yaozhou Kiln, Shaanxi Science and Technology Press, Xi'an, 2000.
- [3] Z.X. Zhuo, A study of Chai kiln, Collectors (2001) 2–9.
- [4] X.Q. Chen, J.Z. Li, R.F. Huang, S.P. Chen, Z.X. Zhuo, B.R. Du, Tang dynasty Yaozhou celadon and black glazed wares, Chin. Ceram. (1990) 57–62.
- [5] G.Z. Li, P.Y. Guan, A study on Yaozhou celadon, J. Chin. Ceram. Soc. 4 (1979) 360–369.
- [6] T.Q. Zhu, H. Huang, H.M. Wang, L.M. Hu, X.B. Yi, Comparison of celadon from the Yaozhou and Xicun kilns in the Northern Song Dynasty of China by X-ray fluorescence and microscopy, J. Archaeol. Sci. 38 (2011) 3134–3140.
- [7] H.J. Lou, J.Z. Li, L.M. Gao, The criterion for compartmentalizing the Chinese ancient glaze and its application in research of ancient glaze, J. Chin. Ceram. Soc. (1995) 50–54.
- [8] X.S. Cheng, S.J. Ke, Q.H. Wang, H. Wang, A.Z. Shui, P.A. Liu, Characterization of transparent glaze for single-crystalline anorthite porcelain, Ceram. Int. 38 (2012) 4901–4908.
- [9] H.W. Nesbitt, G.M. Bancroft, G.S. Henderson, R. Ho, K.N. Dalby, Y. Huang, Z. Yan, Bridging, non-bridging and free (O^{2-}) oxygen in Na_2O - SiO_2 glasses: an X-ray Photoelectron Spectroscopic (XPS) and Nuclear Magnetic Resonance (NMR) study, J. Non-Cryst. Solids 357 (2011) 170–180.
- [10] T. Yamashita, P. Hayes, Analysis of XPS spectra of Fe^{2+} and Fe^{3+} ions in oxide materials, Appl. Surf. Sci. 254 (2008) 2441–2449.
- [11] M. Omran, T. Fabritius, A.M. Elmahdy, N.A. Abdel-Khalek, M. El-Aref, A. Elmanawi, XPS and FTIR spectroscopic study on microwave treated high phosphorus iron ore, Appl. Surf. Sci. 345 (2015) 127–140.
- [12] C.W. Zhang, The structural analysis and coordination discussion on Iron-Ion tinting principle in iron oxide containing glass, Glass Enamel 32 (2004) 38–42.
- [13] W.H. Jiang, Q.L. Liao, Effect of compositions on the microstructure and surface properties of phase separation-crystallization opacified glazes, J. Chin. Ceram. Soc. 35 (2007) 230–235.
- [14] W.D. Li, J.Z. Li, Z.Q. Deng, J. Wu, J.K. Guo, Study on Ru ware glaze of the Northern Song dynasty: one of the earliest crystalline-phase separated glazes in ancient China, Ceram. Int. 31 (2005) 487–494.
- [15] X.M. Wang, The aesthetic and style transformation of Yaozhou celadon, Sichuan Cultural Relics, 2009, pp. 49–54.
- [16] S. Kinoshita, S. Yoshioka, Structural colors in nature: the role of regularity and irregularity in the structure, ChemPhysChem 6 (8) (2005) 1442–1459.
- [17] Y. Takeoka, Angle-independent structural coloured amorphous arrays, J. Mater. Chem. 22 (2012) (2012) 23299–23309.
- [18] Y.M. Yang, M. Feng, X. Ling, Z.W. Mao, C.S. Wang, X.M. Sun, M.S. Guo, Microstructural analysis of the color-generating mechanism in Ru ware, modern copies and its differentiation with Jun ware, J. Archaeol. Sci. 32 (2005) 301–310.
- [19] K. Chung, S. Yu, C.J. Heo, J.W. Shim, S.M. Yang, M.G. Han, H.S. Lee, Y. Jin, S.Y. Lee, N. Park, J.H. Shin, Flexible, angle-independent, structural color reflectors inspired by morpho butterfly wings, Adv. Mater. 24 (2012) 2375–2379.
- [20] K. Ueno, A. Inaba, Y. Sano, M. Kondoh, M. Watanabe, A soft glassy colloidal array in ionic liquid, which exhibits homogeneous, non-brilliant and angle-independent structural colours, Chem. Commun. (2009) 3603–3605.
- [21] Richard O. Prum, Rodolfo H. Torres, A fourier tool for the analysis of coherent light scattering by bio-optical nanostructures, Integr. Comp. Biol. 43 (2003) 591–602.